Joint International Topical Meeting on Mathematics & Computation and Supercomputing in Nuclear Applications (M&C + SNA 2007)
Monterey, California, April 15-19, 2007, on CD-ROM, American Nuclear Society, LaGrange Park, IL (2007)

COMPUTATIONAL PHYSICS OF PHOTON SCIENCE

Mitsuru Yamagiwa, Sergei Bulanov, Timur Esirkepov, James Koga, Tomohito Otobe, and Toshiki Tajima
Japan Atomic Energy Agency
8-1 Umemidai, Kizu, Kyoto 619-0215, Japan
yamagiwa.mitsuru@jaea.go.jp; bulanov.sergei@jaea.go.jp; timur.esirkepov@jaea.go.jp;
koga.james@jaea.go.jp; otobe.tomohito@jaea.go.jp; tajima.toshiki@jaea.go.jp

ABSTRACT

We study laser-matter interactions numerically by using massively parallel computers. The ion acceleration from a double layer target driven by a laser pulse with intensities $I = 10^{20}$-10^{22} W/cm^2 $\times$ $(\mu m/\lambda)^2$ is investigated via multi-parametric particle-in-cell (PIC) simulations. For targets over a wide range of thicknesses l and densities n_e, at a given intensity, the highest ion energy gain occurs for a certain electron areal target density $\sigma = n_e\, l$, which is proportional to the square root of the intensity. It is also found that proton energies in the range of 200 MeV required for deep cancer therapy may possibly be achieved with high power lasers close to petawatt levels. Also reported are simulations of laser wake field acceleration of electrons and photons and laser and neutral gas interaction. Furthermore a first-principle calculation is described for the electron excitation of transparent material under an intense laser field showing that breakdown of the dielectric occurs under the intense laser field and that diamond behaves like a metal.

Key Words: PIC simulation, Laser, Acceleration, First-principle calculation, Electron excitation

1. INTRODUCTION

The research objective of the Advanced Photon Research Center (APRC) of the Japan Atomic Energy Agency (JAEA) is the development of novel radiation sources with high performance and their application using advanced lasers. Utilizing these lasers, APRC also seeks the generation and application of high energy particles and X-rays. These advanced lasers producing highly energetic particles and photons have distinctive characteristics such as high intensity, high coherency, and short pulse, which are different from conventional radiation.

When a relativistically intense ultra-short pulse laser is irradiated onto a gas or a solid target, a high energy density plasma is generated and in an extremely short time various phenomena occur which up till now were not expected. Inside matter irradiated with intense lasers, ultra-high pressure is realized and energetic photons and particles are generated. Fast electrons also excite strong electromagnetic fields.

Optimizing and establishing relevant experimental conditions by simulation has become invaluable because the elucidation of experimental research is difficult due to the fact that the ultra-high acceleration, ultra-high density, and ultra-intense electromagnetic phenomena which arise over extremely short timescales are strongly nonlinear complex phenomena. So, large scale

simulation which utilizes supercomputers is essential for guiding and aiding experimental research.

2. MASSIVELY PARALLEL COMPUTATION OF LASER-MATTER INTERACTION

We use the supercomputer HP Alpha Server SC ES40 (720 CPU's) at JAEA-Kansai and the supercomputer SGI Altix 3900 Bx2 (2048 CPU's) at JAEA-Tokai. Some of our recent activities on the interaction of intense lasers with neutral gas, plasma, and solid are as follows: In order to study the detailed propagation dynamics of high-power short-pulse laser pulses in neutral gases, which is a surprisingly complex phenomenon, a code has been developed which explicitly solves Maxwell's equations including the finite response time background neutral gas polarization and optical field ionization. In large scale two dimensional simulations of a high power laser pulse propagating in hydrogen-like gas the generation of ultra-broadband white light, the so-called super-continuum generation, has been observed [1]. Electron acceleration with a high-intensity short-pulse laser propagating through an underdense plasma layer has also been studied by two-dimensional (2D) particle-in-cell (PIC) simulation, solving Maxwell's equations along with the particle motion of both the electrons and ions. The electron density structure in the plasma and the high energy electron distribution have been analyzed. Dramatic changes of the density structure occur with cavity and bunch formation by the increase of the laser intensity. A fast electron component well confined in phase space appears, leading to a quasi-monoenergetic electron distribution [2, 3]. Furthermore, we have carried out multi-parametric 2D PIC simulations of the laser-driven ion acceleration during the interaction of a relativistically strong laser pulse with a plasma slab [4]. A first-principle calculation, solving the Kohn-Sham equation based on the density functional theory, for the study of electron excitation of transparent material under an intense laser field is also under investigation [5]. In the following we describe results of these and related works.

2.1. Multi-Parametric PIC Simulations of Laser Ion Acceleration Scaling Laws

Due to the laser irradiation of a target, high energy electrons are generated. As a result, an electrostatic field is induced and ions can be efficiently accelerated. For the double layer target, which is composed of a coating of light matter (such as hydrogen) on the back side of a thin metal film target, the proton beam has good directionality and a quasi-monoenergetic spectrum [6, 7]. Currently proton acceleration experiments using high power lasers close to petawatt levels are going on vigorously all over the world with the aim of a compact cancer therapy machine. Finding the optimum conditions for the laser parameters and target designs of micron order thickness only by experiments is, however, very difficult. Therefore, the maximum proton energy is predicted and the dependence on the laser pulse and the target is studied for laser irradiation on a target from which protons originate, by using supercomputers.

We performed multi-parametric 2D PIC simulations to investigate the scaling laws of the intense laser-driven ion acceleration during the interaction of a short relativistically strong laser pulse with a thin overdense plasma slab [4]. The use was made of the code REMP (Relativistic Electro-Magnetic Particle-mesh code) which is massively-parallel and fully vectorized and is designed to work in 2D and 3D geometries [8].

The aim was to define the regions of the laser and plasma parameters in which the ion energy is maximum, the ion energy spread is minimum and laser-to-ion energy transformation efficiency is significant. In particular, we were looking for the necessary conditions to get ions with 200–300 MeV per nucleon, which is necessary for hadron therapy. We used the double-layer target scheme as a method which allows us to obtain a quasi-monoenergetic ion beam. We found that the most critical laser and plasma parameters are the laser amplitude $a=eE/m_e\omega c$, target plasma density n_e and target thickness l. The laser pulse intensity varied in the range $I=10^{20}$–10^{22} W/cm$^2\times(\lambda/\mu m)^2$, the target density n_e – from 1 n_{cr} to 100 n_{cr}, and the target thickness – from 0.1λ to 5λ, where n_{cr} is plasma critical density and λ is wavelength of laser radiation. Figure 1 shows the proton energy with the laser intensity and the target thickness and number density as parameters. Contour lines of the proton energy are plotted in the plane of the laser electric field (a) and the target areal density (σ) or the product of the thickness and the number density. We found that the quickest energy growth rate and thus the largest final energy occur at a certain areal density $\sigma = n_e\, l$, where the optimum σ depends on laser pulse amplitude a quasi-linearly. At each fixed maximum ion energy E_{max} there is minimum amplitude a which gives this E_{max}. In the acceleration mechanism for small thicknesses l and large densities n_e the laser pulse sweeps almost all electrons away and the resulting electrostatic field accelerates ions. For large thicknesses l and small densities n_e the laser pulse shifts and heats electrons, generates strong quasi-static magnetic fields inside the plasma and the corresponding magnetic pressure causes ion acceleration. We found that in the case of thin targets and optimal laser pulse duration, the ion maximum energy scales as the square root of the laser pulse power. We also demonstrated that when the radiation pressure of the laser field becomes dominant, the ion maximum energy becomes proportional to the laser pulse energy.

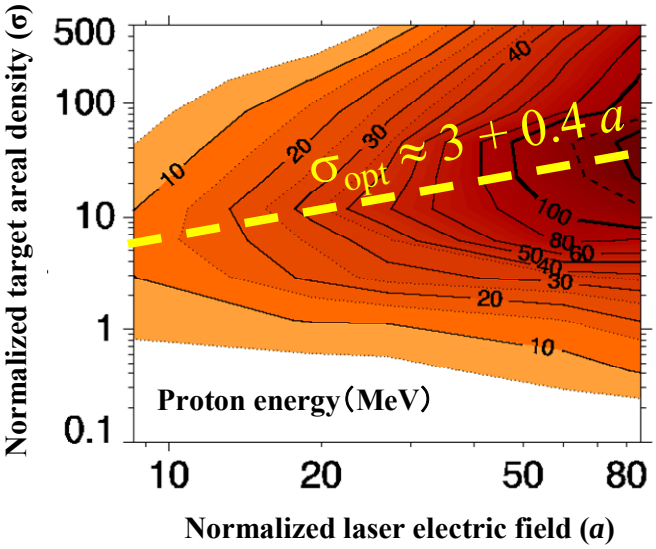

Figure 1. Proton energy in the plane of the laser electric field (a) and the target areal density (σ). a = 8.5 (λ/1μm) $(I/10^{20}$ W/cm$^2)^{1/2}$; λ the laser wavelength; I the laser intensity. $\sigma = (l/\lambda)\,(n_e/n_c)$; l the target thickness; n_e the electron density; n_c the critical density at which the laser pulse is reflected.

2.2. PIC Simulations of Laser Wake Field Acceleration of Electrons and Photons

Ultra-short pulse laser irradiation on an underdense plasma can excite a wake field, i.e., a longitudinal plasma wave with the electric field parallel to the laser propagation and with a phase velocity equal to the group velocity of the laser pulse [9]. The wake field can trap relativistic electrons injected with the speed close to its phase velocity. The trapped electrons gain a substantial amount of energy when they are accelerated forwards.

We analyzed the basic properties of the electron acceleration injected due to the wave breaking into the first period of the wake plasma wave left in an underdense plasma behind the ultra-short laser pulse. The transverse breaking regime accounts for the finite size electron bunch formation. It was found that in the first wake period there are two separatrices (they are the inner and the outer separatrix) that separate transient and trapped particle trajectories in the phase plane. The electrons moving along the trajectories confined in between the inner and the outer separatrix have their velocity greater than the group velocity of the laser pulse. The energy spectrum of the electrons at the top of the separatrix has a typical inverse square root form with a maximum and a sharp cut at the maximal energy. We called this energy spectrum the "quasi-monoenergetic spectrum", because the actual energy width is of the same order as the maximal energy. Transverse oscillations of the electrons have slowly varying amplitude and frequency. Their magnitude determines the transverse emittance of fast electrons. It was shown that for laser pulse lengths above the plasma wake wavelength the wake field accelerated electrons are further accelerated by the electromagnetic wave [10].

Large upshift of frequency of light due to reflection from the breaking wake wave in tenuous plasma is also expected. This "Flying mirror" concept was suggested in Ref. [11] and can be sketched as follows. In a plasma wake wave generated by a relativistically strong laser pulse, modulations of the electron density naturally and robustly take the shape of paraboloidal dense shells, separated by evacuated regions, moving almost at the speed of light. When another counter-propagating laser pulse is sent to the wake wave, it is partially reflected from the shells, acting as relativistic flying semi-transparent mirrors. The reflected radiation is frequency-upshifted due to the double Doppler effect and focused due to the paraboloidal shape of the shells, caused by the relativistic dependence of the plasma frequency on the wake wave amplitude. This leads to the possibility of very strong pulse compression and extreme light intensification.

We performed a preliminary calculation for the "Flying mirror" experiment. We found that the region of parameters favorable for the "Flying mirror" experiment overlaps with the region necessary for good generation of electron bunches. With the available laser, the self-focusing regime is necessary for the successful "Flying mirror" experiment. In the favorable region of parameters, the frequency upshift is visible at all angles from 0 to 90°. The main part of the energy is emitted in the angle inversely proportional to square root of the plasma density.

2.3. High Intensity Ultra-Short Pulse Laser and Neutral Gas Interaction Research

Since the advent of high power short pulse lasers, there has been a renewed interest in the propagation dynamics of high power laser pulses in neutral gases. In our laboratory super-

continuum generation with a total blue-shift of a laser pulse with initial focusing, which is fixed and independent of the gas, has been observed [12]. However, the propagation dynamics and light shift mechanism are not clearly understood. We directly solve Maxwell's equations and automatically include higher order gas polarization. We study the generation of long plasma channel formation by high irradiance laser pulses propagating in neutral gases and determine the physical mechanisms by which super-continuum radiation occurs and how it is influenced by initial focusing of the laser pulse.

Super-continuum radiation has been observed in experiments involving weakly focused high power lasers propagating in neutral gases and has been reproduced in simulations using the envelope and the unidirectional optical pulse propagation approximation. In order to study these types of problems with a minimal amount of approximation we explicitly solve in two dimensions Maxwell's equations, the background neutral gas polarization, and optical field ionization by the laser pulse. This requires much higher resolution in space and time which is overcome by using massively parallel computers. Figure 2 shows the laser pulse after it has propagated 2.4 mm in the gas with a) no initial focusing and b) initial focusing. The simulation box is moving to the right with the laser pulse at nearly the speed of light. The laser pulse in the initial focusing case is spreading out in the y direction faster than in the non-focusing case. For the first time we have simulated the effect of the initial focusing on the change in the laser pulse spectrum. Figure 3 shows power spectra of the laser pulse taken at 2.4 mm propagation distance for no initial focusing (red line) and initial focusing (blue line). With initial focusing the spectrum of the laser pulse is shifted towards higher wave numbers, k/k_0, than in the no initial focusing case. This indicates that initial focusing plays a role in the spectral shifting of the laser pulse. This allows the beginning of the confirmation of experimental results.

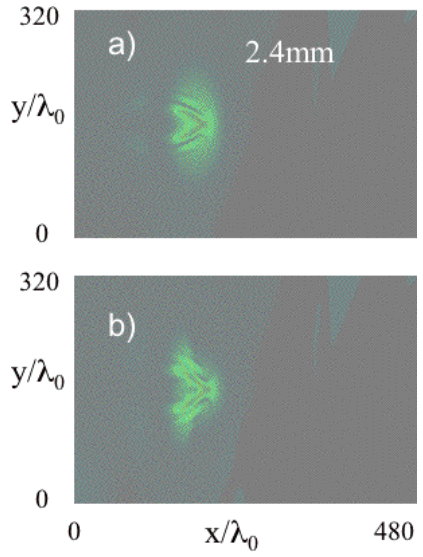

Figure 2. Laser propagation in neutral gas. a) No initial focusing and b) initial focusing.

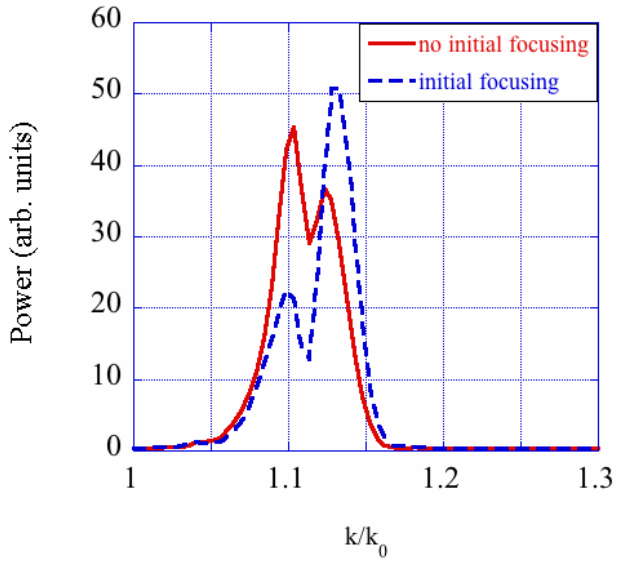

Figure 3. The power spectra of the laser pulses with no initial focusing (red line) and initial focusing (blue line).

2.4. First-Principle Calculation for Electron Dynamics of Diamond under the Intense Laser Field

The interaction between intense lasers and condensed matter has attracted much attention towards the fundamental and applied aspects of this interaction. However, theoretical investigations have not been sufficient enough to clarify the electron dynamics and excitation under the intense laser field. We study the electron non-linear dynamics and excitation with the time-dependent density functional theory (TD-DFT).

Bertsch *et al.* presented the real-time and real-space description of the time-dependent Kohn-Sham (TD-KS) equation for an infinite periodic system and showed the dielectric functions of lithium and diamond by simulating the electron dynamics [13]. We express the uniform electric field with a spatially uniform, time-dependent vector potential to apply Bloch's theorem to the TD-KS equation. The equation for the time-dependent Kohn-Sham orbital is given by

$$i\hbar\frac{\partial\psi_{n\mathbf{k}}(\mathbf{r},t)}{\partial t}=\left\{\frac{1}{2m}\left(\mathbf{p}+\frac{e}{c}\mathbf{A}_{\mathbf{tot}}(t)\right)^2+V_{loc}(\mathbf{r})+\hat{V}_{nonloc}(\mathbf{r},\mathbf{r}')\right\}\psi_{n\mathbf{k}}(\mathbf{r},t) \tag{1}$$

where $\psi_{n\mathbf{k}}(\mathbf{r},t)$ is the time-dependent Kohn-Sham orbital for the band n and the Bloch's momentum $\mathbf{k}$. $V_{loc}(\mathbf{r})$ and $\hat{V}_{nonloc}(\mathbf{r},\mathbf{r}')$ are, respectively, the local and non-local parts of the potential. The local potential is the electron-ion potential, Hartree potential, and exchange-correlation potential. The non-local potential is the non-local part of pseudopotential. In our calculation, we employ the norm-conserving pseudopotential and the local density approximation (LDA) for the exchange-correlation potential. The vector potential $\mathbf{A}_{\mathbf{tot}}(t)$ is constructed by the laser $\mathbf{A}_{laser}(t)$ and the induced $\mathbf{A}_{induced}(t)$ fields,

$$\mathbf{A}_{\mathbf{tot}}(t)=\mathbf{A}_{laser}(t)+\mathbf{A}_{induced}(t) \tag{2}$$

The induced field reflects the screening field inside the material caused by surface charges. The time evolution of the induced field is calculated from the current inside the unit cell,

$$\frac{d^2\mathbf{A}_{\mathbf{induced}}(t)}{dt^2}=\frac{4\pi c}{\Omega}\mathbf{J}(t) \tag{3}$$

Where $\mathbf{J}(t)$ is the electron current and Ω is the volume of the unit cell.

We discretize the unit cell into a uniform mesh to represent the wave function and the Hamiltonian. We employ a higher-order finite-difference scheme, taking 13 points for one direction to approximate the Laplacian operator and the nabla. The treatment of the non-local pseudopotential was explained in detail in Ref. [13]. From the wave function at time t, $\psi_{n\mathbf{k}}(\mathbf{r},t)$, we construct the induced vector potential and the Hamiltonian. The short-time

evolution of the wave function is approximately achieved by this Hamiltonian, $\hat{H}(t)$. We make a Taylor expansion of the time evolution operator,

$$\psi_{n\mathbf{k}}(\mathbf{r},t+\delta t) \approx \exp\left[-\frac{i}{\hbar}\delta t\hat{H}(t)\right]\psi_{n\mathbf{k}}(\mathbf{r},t) \approx \sum_{k=0}^{4}\frac{1}{k!}\left(-\frac{i}{\hbar}\delta t\hat{H}(t)\right)^{k}\psi_{n\mathbf{k}}(\mathbf{r},t) \quad (4)$$

We confirmed the convergence for the artificial parameters (mesh size, Bloch's momentum sampling, and the time step). We find convergence at a mesh size of 0.35 a.u. (5832 points), a Bloch's momentum sampling of 4096 points, and a time step of 2.419×10^{-4} fs for the laser frequency $\hbar\omega$=0.11 a.u..

Figure 4 shows the electric field of the laser (dashed line) and the total field in the bulk system (solid line). We set the laser irradiance at 1×10^{14} W/cm^2, the frequency at 0.11 a.u., and the pulse length at 661 a.u.. The field induced by the surface charge reduces the external laser field significantly and the realistic field (total field) becomes weak. The total field follows the external field. Figure 5 shows the case for the laser irradiance of 1×10^{15} W/cm^2. The total field shows a peak after the peak of the laser field. Furthermore, the total field does not follow the laser field after the laser field peaks and still exists after the laser pulse, which is a spontaneous oscillation of electrons. Figure 6 shows the case of 1×10^{16} W/cm^2. After the peak intensity, the direction of the total field is opposite to that of the laser field, indicating strong suppression of the laser field because of strong electron excitation from the valence band to the conduction band occurred in the intense laser field. This strong suppression reflects the breakdown of the dielectric. We cannot realize the spontaneous oscillation after the laser pulse as in the case of 1×10^{15} W/cm^2.

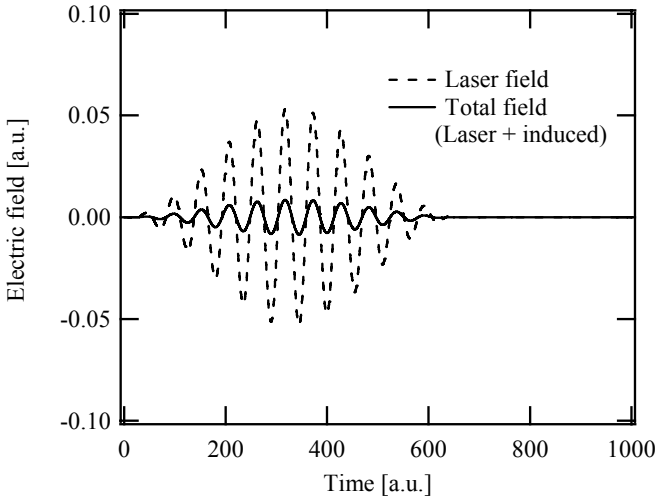

Figure 4. Laser field (dashed line) and the total field (solid line) inside of the bulk diamond. The laser peak irradiance is 1×10^{14} W/cm^2.

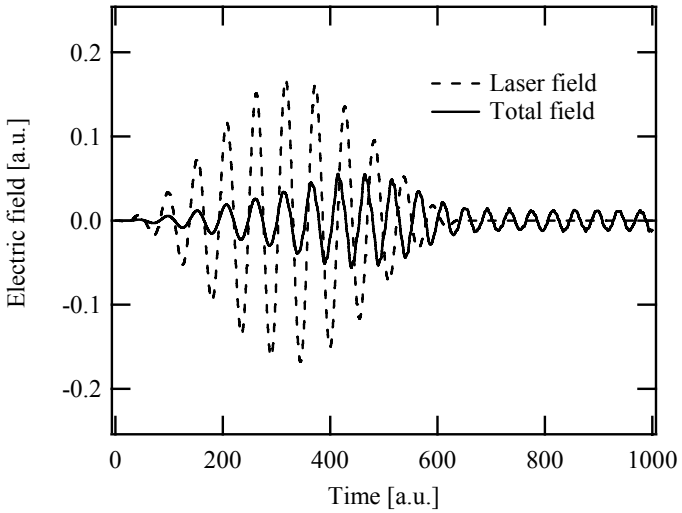

Figure 5. The same as Figure 4 except the laser peak irradiance is 1×10^{15} W/cm^2.

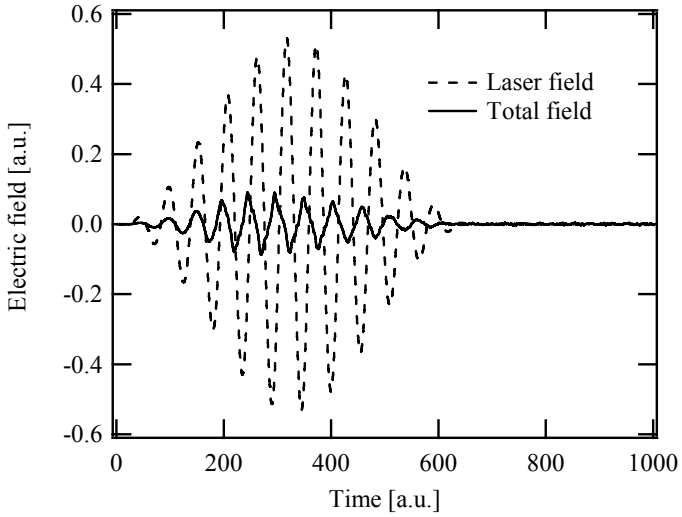

Figure 6. The same as Figure 4 except the laser peak irradiance is 1×10^{16} W/cm^2.

We have investigated the electron dynamics and excitation of diamond under an intense laser field. This is the first study of the first-principle calculation for the non-linear response of electrons in the bulk system. We have found that a shift of the electron oscillation occurs from the external laser field and that the energy absorption becomes substantial as the laser irradiance increases.

3. CONCLUSIONS

We have shown some of our recent simulation activities on the interaction of intense lasers with plasma, neutral gas, and solid. Using multi-parametric two-dimensional (2D) Particle-in-Cell (PIC) simulations, we investigated the scaling laws of the intense laser-driven ion acceleration and found that to attain a given proton energy the necessary laser electric field strength (a) can be minimized by appropriately choosing the target areal density (σ) and that the optimum relation between a and σ is given by the scaling law of $\sigma=\sigma_{opt}\sim3+0.4\ a$. As for laser wake field acceleration of electrons and photons, simulation research to aid the "Flying mirror" experiment is going on and a preliminary calculation revealed the optimal condition for the intersection point of the source and driver pulses and confirmed that the effect of reflection must be searched at the same plasma densities at which good electron acceleration is seen. We also studied the generation of plasma formation by high irradiance laser pulses propagating in neutral gases by directly solving Maxwell's equations and automatically including higher order gas polarization and found that with initial focusing the spectrum of the laser pulse is shifted towards higher wave numbers than in the no initial focusing case. Furthermore we studied the electron excitation of transparent material under an intense laser field through the first-principle calculation based on the time dependent density functional theory (TD-DFT). We found that the field induced by the surface charge leads to reduction of the total field and that a shift of the electron oscillation occurs from the external laser field as the laser irradiance increases, which may show signs of metallization of the diamond.

ACKNOWLEDGMENTS

This work was in part supported by MEXT, Grant-in Aid for Creative Scientific Research (15GS0214), Specially Promoted Research (15002013), and JST-CREST. M.Y. and T.O. are grateful for valuable discussions with K. Yabana, J. Iwata, and T. Nakatsukasa. The simulations were carried out on the HP Alpha Server SC ES40 at JAEA-Kansai and the SGI Altix 3900 Bx2 at JAEA-Tokai.

REFERENCES

1. J. Koga, "Observation of supercontinuum generation in the direct simulation of an intense laser pulse propagating in a neutral gas," *Phys. Rev. E*, **70**, pp. 056404-1-056404-5 (2004).
2. S.V. Bulanov, M. Yamagiwa, T.Zh. Esirkepov, et al., "Spectral and dynamical features of the electron bunch accelerated by a short-pulse high intensity laser in an underdense plasma," *Phys. Plasmas*, **12**, pp. 073103-1-073103-11 (2005).
3. M. Yamagiwa, S.V. Bulanov, T.Zh. Esirkepov, et al., "Simulation of electron bunch generation by an ultrashort-pulse high-intensity laser-driven wakefield," *Laser Phys.*, **16**, pp. 252-258 (2006).
4. T. Esirkepov, M. Yamagiwa, T. Tajima, "Laser ion acceleration scaling laws seen in multiparametric PIC simulations," *Phys. Rev. Lett.*, **96**, pp. 105001-1-105001-4 (2006).
5. T. Otobe, K. Yabana, J. Iwata, et al., "First-principle calculation for interaction between many electrons system and laser field," International Wilhelm and Else Heraeus Summerschool, Few-body dynamics in atomic and molecular systems, Wittenberg (2006).
6. S.V. Bulanov, V.S. Khoroshkov, "Feasibility of using laser ion accelerators in proton therapy," *Plasma Phys. Rep.*, **28**, pp. 453-456 (2002).

7. T.Zh. Esirkepov, S.V. Bulanov, K. Nishihara, et al., “Proposed double-layer target for the generation of high-quality laser-accelerated ion beams,” *Phys. Rev. Lett*., **89**, pp. 175003-1-175003-4 (2002).
8. T.Zh. Esirkepov, “Exact charge conservation scheme for particle-in-cell simulation with an arbitrary form-factor,” *Comp. Phys. Commu.*, **135**, pp. 144-153 (2001).
9. T. Tajima, J.M. Dawson, “Laser electron accelerator,” *Phys. Rev. Lett.*, **43**, pp. 267-270 (1979).
10. T. Esirkeov, S.V. Bulanov, M. Yamagiwa, T. Tajima, ”Electron, positron, and photon wakefield acceleration: Trapping, wake overtaking and ponderomotive acceleration,” *Phys. Rev. Lett.*, **96**, pp. 014803-1-014803-4 (2006).
11. S.V. Bulanov, T. Esirkepov, T. Tajima, “Light intensification towards the Schwinger limit,” *Phys. Rev. Lett.*, **91**, pp. 085001-1-085001-4 (2003).
12. J.K. Koga, N. Naumova, M. Kando, et al., “Fixed blueshift of high intensity short pulse lasers propagating in gas chambers,” *Phys. Plasmas*, **7**, pp. 5223-5231 (2000).
13. G.F. Bertsch, J.-I. Iwata, A. Rubio, K. Yabana, “Real-space, real-time method for the dielectric function,” *Phys. Rev. B*, **62**, pp. 7998-8002 (2000).